NUMERICAL INVESTIGATION OF THE THERMOHYDRAULIC PERFORMANCE OF DOUBLE-PIPE HEAT EXCHANGERS UNDER OCEAN MOTIONS

by

Zixiong ZHU[a], Hanzhong TAO[a], Yannan LI[a*], Mengmeng LIU[a], and Yongqiang CHEN[b]

[a] School of Energy Science and Engineering,
Nanjing Tech University, Jiangsu, China
[b] Zhejiangxianchuang Energy Technology Co., Ltd,
Jinhua, Zhejiang, China

Original scientific paper
https://doi.org/10.2298/TSCI230201125Z

In this paper, the finite volume method was used to numerically study the heat transfer and flow of double-pipe heat exchangers (DPHE) under static and ocean motion conditions. The ocean motion is simplified as a harmonic oscillation with the center of the DPHE as the axis of rotation. In addition the flow direction and the inlet Reynolds number, the effects of amplitude and period ontal heat transfer coefficient, pump power and thermal performance factor were also analyzed quantitatively. The results showed that as the heat exchanger oscillates, the total heat transfer coefficient, and pump power exhibit a periodic change and the period is half of the oscillating period of the heat exchanger. The total heat transfer coefficients for all oscillating DPHE are higher compared to static conditions, reaching a maximum improvement of 9.84% at low Reynolds numbers. The total heat transfer coefficient and pump power of DPHE under oscillation are significantly regular, positively correlated with amplitude and negatively correlated with period. When the amplitude exceeds 0.5 rad/s, the oscillatory condition has thermal performance improvement for the oscillating DPHE with the inner tube with low Reynolds number and the outer tube with high Reynolds number. In the optimum condition, the thermal performance of the inner and outer tubes is improved by 5.01% and 1.48%, respectively. The thermal performance coefficient of DPHE hardly changed when the period exceeded 5 seconds. The results herein provide a theoretical basis for predicting the development of offshore double-pipe heat exchange equipment.

Key words: *DPHE, period oscillation motion, heat transfer enhancement, thermal performance*

Introduction

Double-pipe heat exchangers are coaxial DPHE composed of two different sizes of standard tubes [1]. Due to the reliable performance, they are widely used in various fields, including on ocean ships and offshore floating platforms. Due to the action of waves and sea breezes, offshore equipment will produce unstable motion which is complex and can be roughly divided into three axes *X*, *Y*, and *Z*, as shown in fig. 1 [2, 3]. This means that the equipment on board (including the DPHE) work under an oscillation state, so it is necessary to consider the

* Corresponding author, e-mail: liyannan@njtech.edu.cn

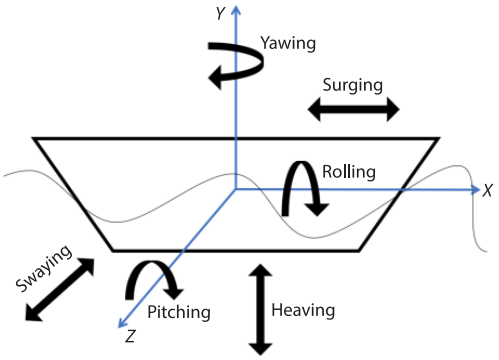

Figure 1. The sketch of the three axis of ocean motion [2, 3]

influence of ocean motions on the heat transfer performance of DPHE. However, the current researches on DPHE and its heat transfer under ocean motions are segregated.

On one hand, researches on DPHE considered onshore stationary applications and they focused on changing the pipe geometry of DPHE [4, 5], adding fins [6] and coiled wire [7] in the pipe, using nanofluids [8, 9], and metallic foams [10] and other aspects to improve the heat exchange thermal performance.

On the other hand, the researches on flow and heat transfer under ocean conditions focused on the flow and convective heat transfer in a single tube, rather than the overall thermohydraulic performance of a heat exchanger. These researches can be divided into experimental and simulation studies.

Pendyala *et al.* [11] conducted an experimental study on the flow and pressure drop in the low frequency (range of 0.1-1 Hz) oscillation vertical tube. When the Reynolds number was in the range of 500-6500, the fluctuation of the flow velocity in the tube mainly depends on the Reynolds number, and the correlation between the Reynolds number and the average flow velocity and pressure drop is established. Tian *et al.* [12] studied the single-phase natural circulation heat transfer in narrow, vertical, and rectangular channels under rolling motion conditions, and compared it with that under static conditions. The results showed that the natural circulation flow changed periodically under rolling conditions, and the heat transfer was enhanced, and the instantaneous Nusselt number under rolling motion conditions predicted by static thermal hydraulic parameters was established. Wang *et al.* [13] studied the single-phase forced circulation heat transfer of a circular tube under rolling motion and found that the larger the average circulating flow rate and rolling period, the smaller the pulsation amplitude of Reynolds and Nusselt numbers. Chong *et al.* [14] used the Sieder-Tate correlation in the laminar flow region and the Gnielinski correlation in the turbulent flow region predict the time-averaged Nusselt number under rolling conditions, and developed a new correlation predict the instantaneous heat transfer characteristics of the fluid under rolling motion conditions. The correlations under rolling motion established according to the aforementioned experimental research provides a valuable basis for numerical simulation.

Compared to experimental research, numerical simulation may involve lower costs and higher accuracy. Bagherzadeh and Javadi [15] conducted a 2-D study of the flow field around a circular cylinder with swing thin plates. Rahman and Tafti [16] conducted a numerical simulation analysis on the heat transfer enhancement characteristics of an oscillating flat plate-fin in the flow field. Yang and Chen [17] performed numerical simulations on the turbulence and heat transfer characteristics of a heating block in the oscillating cylinder channel, and used the Arbitrary Lagrangian-Eulerian method to analyze the time-dependent moving boundary problem of the flow field. Through the visualization of flow field, the vortex structure and Nusselt number distribution caused by fluid oscillation in the heat exchanger at different times were displayed. It was found that eddy current played a key role in enhancing heat transfer. Rui and Tao [18] numerically studied the heat transfer and flow of fluid with constant wall temperature in a tube under periodic cosine oscillation.

According to the aforementioned researches, ocean motion can improve the heat transfer effect in the tube. It is speculated that the thermohydraulic performance of DPHE should be improved under ocean motion, but usually only the enhanced heat transfer in the heat exchange tube is studied, and there is no related study to study the overall performance of DPHE. Therefore, the total thermohydraulic performance of double-pipe heat exchangers under ocean motions which was simplified to a periodic cosine oscillation was numerically studied in this paper. In order to eliminate the influence of flow state on flow and heat transfer performance, the cold and hot fluids in the DPHE were limited to vigorous turbulent flow state.

Model

Physical model

Hashemian *et al.* [4, 19] studied the flow and heat transfer of the improved geometry of the DPHE in the static state only. In this paper, their geometric model of DPHE is used to study the fluid-flow and heat transfer characteristics under oscillating motion. The specific parameters are shown in tab. 1, and the schematic diagram of the geometric model is shown in fig. 2. The boundary conditions for this model use velocity inlet, pressure outlet. The turbulence intensity I = 5%, hydraulic diameter of inner pipe and outer pipe D = 30 mm. All walls of the heat exchanger are non-slip wall conditions. The working fluid is water-liquid and the tube material is steel with thermal conductivity of 16.3 W/mK.

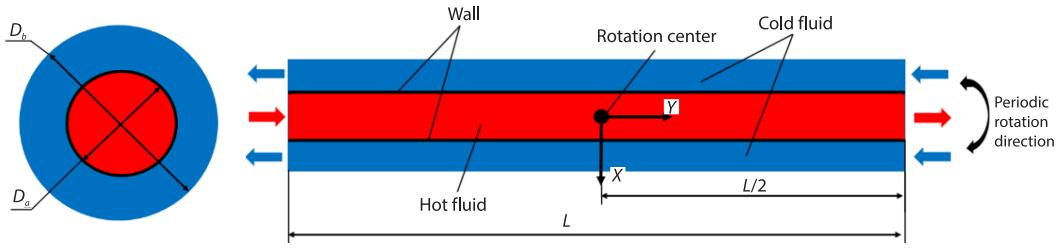

Figure 2. Geometric structure and flow direction of the model

Table 1. The geometry of the tube

Name of parameter	Symbol	Value
The length of the tube	L	500 mm
The diameter of the inner tube	D_a	30 mm
The diameter of the outer tube	D_b	62 mm
The thickness of the inner tube	δ	1 mm

Table 2. Physical parameters of fluid

Parameters	Unit	Hot fluid	Cold fluid
Temperature, t	[K]	325.15	298.15
Density, ρ	[kgm^{-3}]	987.1	997.0
Special heat capacity, c_p	[Jkg^{-1}K^{-1}]	4175	4178.5
Thermal conductivity, λ	[Wm^{-1}K^{-1}]	0.6502	0.6085
Dynamic viscosity, μ	[Pa·s]	$5.33 \cdot 10^{-4}$	$9.03 \cdot 10^{-4}$

In order to facilitate calculation, research and analysis of the model, the following rationalization assumptions are made:

- It is assumed that during the oscillating process, fluids are considered continuous and incompressible, the fluid temperature at the inlet of the tubes is constant and the physical properties are independent of temperature. The specific physical parameters are shown in tab. 2.
- During the transient simulation, the hot and cold fluids remain in an unsteady-state.
- In terms of ship design, due to the long and narrow design of ships and floating platforms, rolling, pitching, and yawing motions are more common. Considering the aforementioned three common oscillatory motions, the single-DoF ocean oscillatory motion is simplified to the cosine law [20].
- In order to characterize the oscillation center of the DPHE, the rotation axis in the DPHE is assumed to be the same as the rotation axis of the ship's motion [21].
- The wall is assumed to be smooth without heat loss, ignoring the effect of buoyancy and gravity is considered on the Z-axis.

Governing equations and turbulence model

The CFD code was used for numerical simulation. According to the previous assumptions, the flow and heat transfer primarily follow the continuity equation, energy equation and momentum equation [22, 23]. The equations are:

- Continuity equation

$$\frac{\partial V_u}{\partial x_u}+\frac{\partial V_v}{\partial x_v}+\frac{\partial V_w}{\partial x_w}=0 \tag{1}$$

- Momentum equation

$$\begin{aligned}
\rho F_u-\frac{\partial p}{\partial x_u}+\mu_e\left(\frac{\partial^2 V_u}{\partial x_u^2}+\frac{\partial^2 V_u}{\partial x_v^2}+\frac{\partial^2 V_u}{\partial x_w^2}\right)-\rho\frac{\mathrm{d}V_u}{\mathrm{d}\tau}=0\\
\rho F_v-\frac{\partial p}{\partial x_v}+\mu_e\left(\frac{\partial^2 V_v}{\partial x_u^2}+\frac{\partial^2 V_v}{\partial x_v^2}+\frac{\partial^2 V_v}{\partial x_w^2}\right)-\rho\frac{\mathrm{d}V_v}{\mathrm{d}\tau}=0\\
\rho F_w-\frac{\partial p}{\partial x_w}+\mu_e\left(\frac{\partial^2 V_w}{\partial x_u^2}+\frac{\partial^2 V_w}{\partial x_v^2}+\frac{\partial^2 V_w}{\partial x_w^2}\right)-\rho\frac{\mathrm{d}V_w}{\mathrm{d}\tau}=0
\end{aligned} \tag{2}$$

- Energy equation:

$$\frac{\partial t}{\partial \tau}+V_u\frac{\partial t}{\partial x_u}+V_v\frac{\partial t}{\partial x_v}+V_w\frac{\partial t}{\partial x_w}-\frac{\lambda}{\rho c_p}\left(\frac{\partial^2 t}{\partial x_u^2}+\frac{\partial^2 t}{\partial x_v^2}+\frac{\partial^2 t}{\partial x_w^2}\right)=0 \tag{3}$$

where V is velocity, u, v, w are the directions of co-ordinates, p and ρ – the pressure and density, μ – the dynamic viscosity, τ – the time, F – the body force and composed of gravity, g, Coriolis force and centripetal force, $F_1=\omega^2 l_s$ (l_s is distance between fluid micelle and oscillation center). Therefore, $F_u=F_{1u}+2\rho\omega\times V$, $F_v=F_{1v}$, $F_w=F_{1w}+$ g, and F_{1u}, F_{1v}, and F_{1w} are the components of the centripetal force on the co-ordinate axis.

In order to ensure the accuracy of turbulence model, the heat transfer coefficient, Nusselt number, and friction coefficient, f, of the solution results of different models (standard k-ε, realizable k-ε, standard k-ω, SST k-ω and Reynolds stress) are compared with Gnielinski equation and Petukhov correlation [24]. The $\mathrm{Re_h}$ is constant at 16668, and the $\mathrm{Re_c}$ are between 9936-36433.

The comparison results are shown in fig. 3. Compared with other turbulence models, the standard k-ε model has the smallest error. The maximum error of Nusselt number between the simulation result and Gnielinski equation is 5.4%, while the maximum error of f between the simulation result and Petukhov correlation is 4.1%. Therefore, the turbulence model adopts the standard k-ε equation (scalable wall function).

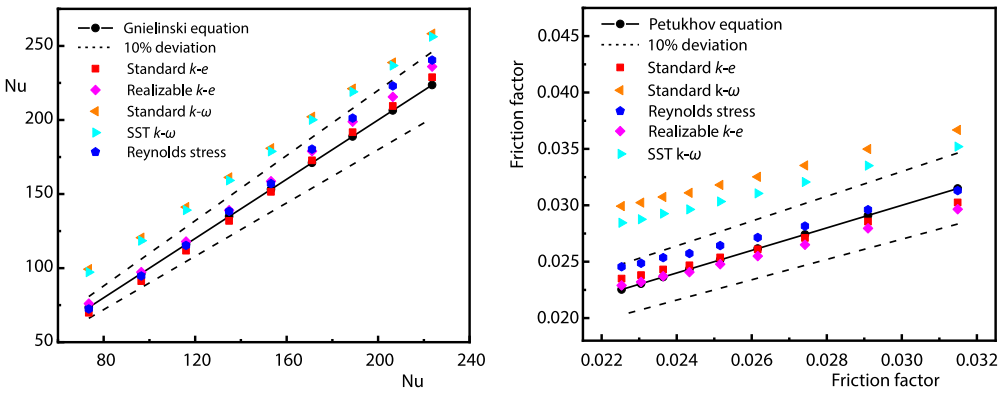

Figure 3. Deviation of the results of each turbulence model with empirical correlation

Independence test

The discretization process of the computational region has a significant influence on the simulation results. In this work, structured hexahedral mesh is generated. Since the change of flow field near the wall needs to be considered, this part of the grid is refined, as shown in fig. 4. The maximum size of the cell is $5 \cdot 10^{-4}$ m, the number of layers is 5, and the growth rate is 1.2. The grids skewness is mainly distributed in the range of 0.02-0.48, the maximum skewness is 0.72 and the thickness of the first layer of the grid immediately above the wall is all less than Y^+. Five different numbers of meshes are generated for mesh independence test. When the grid number exceeds $7.7 \cdot 10^5$, Nusselt number and f increase by just 0.7% and 0.03%, respectively, with the increase in the number of grids, which implies the sufficient mesh number to simultaneously reduce the cost of calculation.

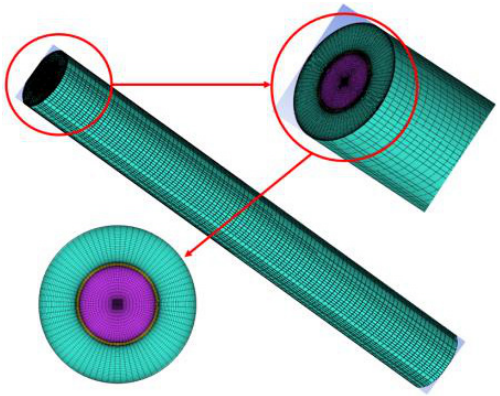

Figure 4. The grid structure of DPHE

Additionally, the numerical simulation's results are significantly influenced by the time step option. At present, Courant number [25, 26] is commonly used to express the relationship between grid size and transient calculation time step. The specific expression is shown in eq. (6). In order to ensure the accuracy of numerical simulation results, the Courant number should be less than 1. Although the smaller time step has a high degree of consistency with the actual value, it will increase the high computational cost at the same time. Considering the calculation time and accuracy, the courant number is set to 0.5 and time step is set to 0.005 second, respectively:

$$Co = \frac{v\Delta\tau}{\Delta x} \tag{4}$$

Numerical method

Parameter definition

For the flow and heat transfer of single DPHE, the total heat transfer coefficient, K, and pump power, P), are important characterization factors. The parameters involved in this study are calculated as follows.

The Reynolds number is calculated:

$$\mathrm{Re} = \frac{\rho V D_\mathrm{e}}{\mu} \tag{5}$$

where ρ is the density, μ – the dynamic viscosity, and V – the inlet velocity. The total heat transfer coefficient K:

$$K = \frac{Q}{S \cdot LMTD} \tag{6}$$

where S is the total heat transfer area of the tube wall and cold water and $LMTD$ – the logarithmic average temperature difference, calculated from eq. (9):

$$LMTD = \frac{\Delta t_1 - \Delta t_2}{\ln\left(\frac{\Delta t_1}{\Delta t_2}\right)} \tag{7}$$

for counter-flow

$$\Delta t_1 = (t_{\mathrm{h,in}} - t_{\mathrm{c,out}}),\ \Delta t_2 = (t_{h,\mathrm{out}} - t_{\mathrm{c,in}}) \tag{8}$$

where $t_{\mathrm{c,in}}$ and $t_{\mathrm{c,out}}$ are the average temperature of the cold water inlet and outlet surface, respectively. Parameters $t_{\mathrm{h,in}}$ and $t_{\mathrm{h,out}}$ are the average temperature of the hot water inlet and outlet surface, respectively.

Heat transfer quantity, Q is defined:

$$Q = \frac{Q_\mathrm{h} + Q_\mathrm{c}}{2} \tag{9}$$

where overall heat transfer quantities of the hot water in the inner pipe and the cold water in the outer pipe are:

$$Q_\mathrm{h} = c_{p,\mathrm{h}} q_{m,\mathrm{h}} (t_{\mathrm{h,in}} - t_{\mathrm{h,out}}),\ Q_\mathrm{c} = c_{p,\mathrm{c}} q_{m,\mathrm{c}} (t_{\mathrm{c,out}} - t_{\mathrm{c,in}}) \tag{10}$$

Pump power, P is defined as:

$$P = (p_{\mathrm{c,in}} - p_{\mathrm{c,out}}) q_{v,\mathrm{c}} + (p_{\mathrm{h,in}} - p_{\mathrm{h,out}}) q_{v,\mathrm{h}} \tag{11}$$

where $p_{\mathrm{c,in}}$ and $p_{\mathrm{c,out}}$ are the average pressure of the cold water inlet and outlet surface, respectively. The $p_{\mathrm{h,in}}$ and $p_{\mathrm{h,out}}$ are the average pressure of the hot water inlet and outlet surface, respectively.

The average K and P per period, $\overline{K}$ and $\overline{P}$ is calculated:

$$\overline{K} = \frac{\int_{\tau_1}^{\tau_2} K \mathrm{d}r}{\tau_2 - \tau_1},\ \overline{P} = \frac{\int_{\tau_1}^{\tau_2} P \mathrm{d}r}{\tau_2 - \tau_1} \tag{12}$$

Nusselt number is by definition:

$$\mathrm{Nu} = \frac{h D_\mathrm{e}}{\lambda} \tag{13}$$

where convective heat transfer coefficients of the hot water in the inner pipe and the cold water in the outer pipe are:

$$h_{\text{inner}} = \frac{Q}{0.5(t_{\text{h,in}} + t_{\text{h,out}}) - t_{\text{wall}}}, \quad h_{\text{outer}} = \frac{Q}{t_{\text{wall}} - 0.5(t_{\text{c,in}} + t_{\text{c,out}})} \tag{14}$$

Friction factor, f is calculated:

$$f = \frac{2d(p_{\text{in}} - p_{\text{out}})}{L\rho V^2} \tag{15}$$

where p_{in} and p_{out} are the average pressure of the corresponding water inlet and outlet surface, respectively.

The simulation schemes

In order to save on computing resources, the static DPHE is initially calculated. After the convergence of the calculation, the heat transfer and flow in the DPHE are now stable. By then writing a user-defined function based on C language, the periodic cosine function is imported into the software to make the stationary DPHE in a periodic cosine oscillation state. The cosine function of the angular velocity of oscillating motion can be expressed:

$$\omega = A\cos\left(\frac{2\pi\tau}{T}\right) \tag{16}$$

where A and T are oscillating amplitude and period, respectively.

Transient solution is used to study the flow and heat transfer of the periodically oscillating DPHE. In this study, the second order FVM is used to solve the governing equations. Under the same calculation accuracy, the SIMPLE algorithm based on pressure and velocity coupling is used to minimize the calculation convergence time, and the interpolation scheme of the pressure equation is of second order [27]. The first-order upwind scheme is used to discretize the turbulent kinetic energy and turbulent dissipation rate, the second-order upwind discretization scheme is used for the momentum equation, and the first-order implicit method is used to discretize the transient formulation. Only the convergence standard of the energy term is set to 10^{-7}, whilst the other convergence standards are set to10^{-6}.

Model validation

In order to check the accuracy of the numerical simulation results, the transient Nusselt number and f of the simulation results are compared with the results of [18]. The comparison results are shown in fig. 5. Compared with [18], the simulation results show that the maximum errors of average Nusselt number and f are within 10%, demonstrating that the simulation results are reliable.

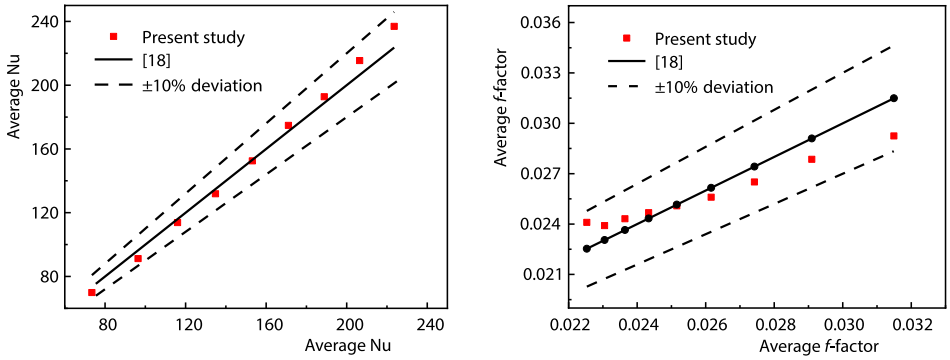

Figure 5. Deviation of present study with [18]

Results and discussions

Transient characteristics of K and P

In the simulation process, the steady-state heat transfer of static DPHE was simulated initially, and when $\tau = 0$ seconds, the DPHE begins oscillating in the form of the periodic cosine function. Figure 6 shows the changes of K and P with flow time at various DPHE oscillating periods in the performance of counter-flow ($Re_c = 23184$, $Re_h = 16668$, $A = 0.5$ rad/s):

- As can be seen, the heat transfer and flow in the DPHE experienced an unstable process at the beginning of periodic motion and then developed into a periodic process. The red line indicated the time required for transient K and P to develop into a periodic motion. When $T = 5$ seconds, 10 seconds, 15 seconds, and 20 seconds, transient K shown periodic characteristics after 2.5 seconds, 2.6 seconds, 2.6 seconds, and 2.6 seconds, respectively, and P illustrated periodic characteristics after 1.9 seconds, 1.9 seconds, 2.5 seconds, and 2.5 seconds, respectively. With the increase in T, whether K or P, the time required to develop to the periodic change state also increased.
- Furthermore, for any T, P required a shorter time than K to reach the periodic motion state, which could be attributed to faster momentum transfers than heat.
- With the periodic oscillation of DPHE, K and P also presented a periodic motion state, and their periods were half of that of DPHE (as shown by the blue line).
- As the DPHE oscillation period increases, K_{max} and P_{max} increases, whilst K_{min} and P_{min} decreases. After T reaches 10 seconds, the values of K_{max}, K_{min}, P_{max}, and P_{min} tend to be constant. When T increased from 5-20 seconds, K_{max} increases from 1286.0-1289.4 W/m^{2}K and the corresponding K_{min} decreases from 1246.1-1233.0 W/m^{2}K. Likewise, P_{max} increases from 0.1902-0.1908 W and P_{min} decreases from 0.1873-0.1859 W.

In general, K_{max} varies little by T, while K_{min} varies more. Furthermore, the ΔK ($\Delta K = K_{max} - K_{min}$) and ΔP ($\Delta P = P_{max} - P_{min}$) were positively correlated with T when T is in the range of 5~20 seconds.

The effect of amplitudes on K and P of DPHE

The total heat transfer coefficient K is an important indicator to evaluate the heat transfer capacity of the heat exchanger. The $\overline{K}$ of a periodically oscillating DPHE is compared with the stationary condition. Figure 7 shows the effect of amplitudes on $\overline{K}$ at nine different Reynold number (counter-flow) when the oscillation $T = 10$ seconds. Noticeably, for the same Re_h, the $\overline{K}$ under oscillating motion was higher than that of the static tube. When $A = 1$ rad/s, the $\overline{K}$ is highest. With the increase of A from 0 to 1 rad/s, $\overline{K}$ increased by 9.84 %, 7.67%, 7.47%, 7.38%, and 7.38% for varying Re_c. However, when $A = 0.25$ rad/s, not all variations of $\overline{K}$ are positive. When $Re_c = 36433$, the maximum decrease in $\overline{K}$ of DPHE is –0.89%. For the same Re_c with different Re_h, the enhancement effect of $\overline{K}$ is diminished. With the increase of A from 0-1 rad/s, $\overline{K}$ increased by 7.47%, 3.55%, 2.46%, 2.15%, and 2.32% for varying Re_h. The aforementioned difference is that when $A = 0.25$ rad/s, the low Re_h number brings about a weakening of heat transfer.

The oscillating motion with amplitude above 0.5 rad/s was found to destroy the boundary-layer of the fluid near the tube wall in section 4.1 and 4.2, enhancing radial heat transfer, and thus the heat transfer was enhanced. When the amplitude is equal to 0.25 rad/s, the effect of oscillatory motion on heat transfer is small and unstable. The improvement in heat transfer to the DPHE caused by periodic oscillation gradually declines as Reynold rises. The improvement of heat transfer is decreasing as the Reynold number increases. This indicates that the fluid-flow with high Reynold number is more difficult to receive perturbations from oscillatory motions.

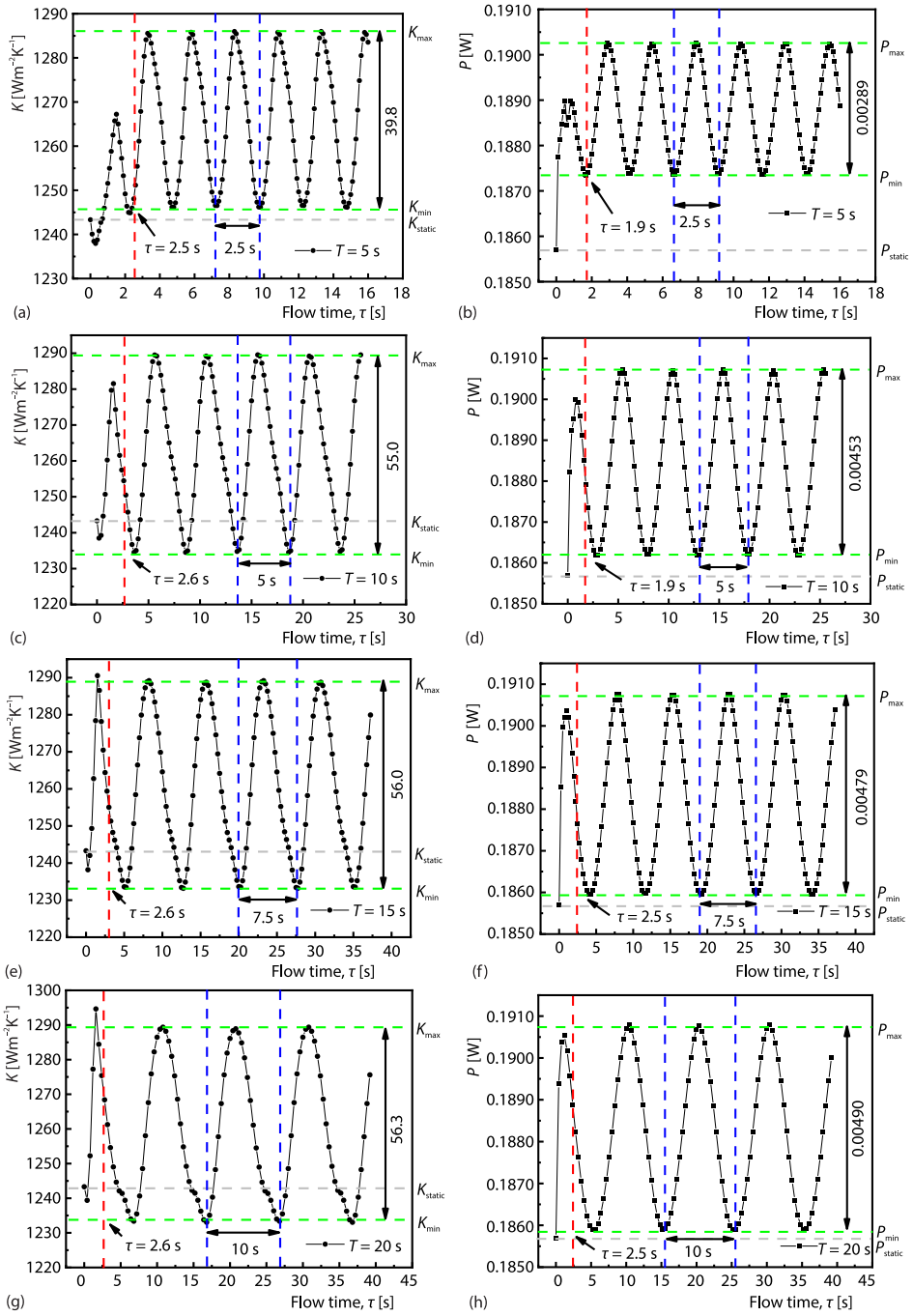

Figure 6. The changers of *K* and *P* with flow time at various DPHE oscillating periods; (a) total heat transfer coefficient when *T* = 5 seconds, (b) pump power when *T* = 5 seconds, (c) total heat transfer coefficient when *T* = 10 seconds, (d) pump power when *T* = 10 seconds, (e) total heat transfer coefficient when *T* = 15 seconds, (f) pump power when *T* = 15 seconds, (g) total heat transfer coefficient when *T* = 20 seconds, and (h) pump power when *T* = 20 seconds

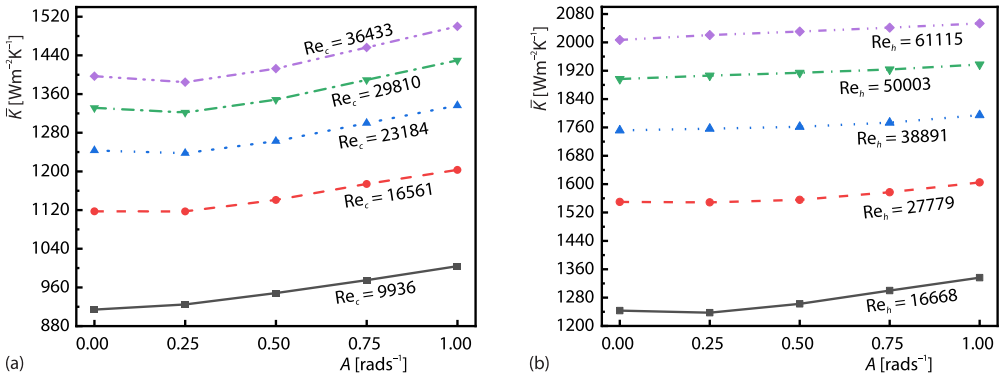

Figure 7. The effect of amplitudes on $\bar{K}$; (a) average total heat transfer coefficient when Re_h = 16668 and (b) average total heat transfer coefficient when Re_c = 23184

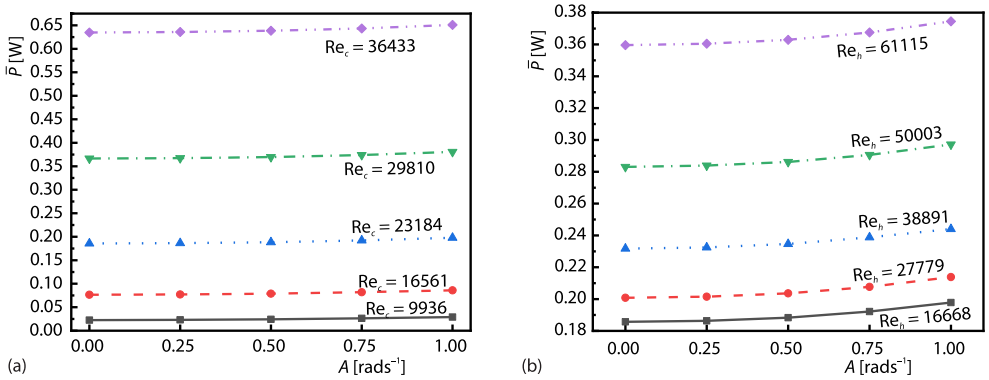

Figure 8. The effect of amplitudes on $\bar{P}$; (a) average pump power when Re_h = 16668 and (b) average pump power when Re_c = 23184

Figure 8 shows the effect of amplitudes on $\bar{P}$ at ten different Reynolds number when the oscillation period T = 10 seconds. The $\bar{P}$ of the DPHE under periodic oscillation is higher than that of the static DPHE, which indicates that the oscillation brought a higher pump power to the heat exchanger. The $\bar{P}$ increases with the increase of A. As the amplitude increased from 0-1 rad/s, the $\bar{P}$ is enhanced by 28.33%, 12.13%, 6.52%, 3.89%, and 2.56 for various Re_c and the $\bar{P}$ is enhanced by 6.52%, 6.46%, 5.65%, 4.97%, and 4.15% for various Re_h. This implied that when Reynolds number was large enough, the effect of additional inertial force on the velocity boundary-layer was relatively reduced. The oscillating motion of heat exchanger would change the additional force on the fluid in the tube, and these forces affected the magnitude of friction pressure drop. When *Re* was low, the oscillation made the fluid in the tube subject to a large additional force and created a large pressure drop and pump power.

The effect of periods on K and P of DPHE

Further to the amplitude, the oscillation period is also a factor that can influence the performance of DPHE. Figure 9 shows the relationship between $\bar{K}$ and various period at ten different Reynold number (A = 0.5 rad/s, counter-flow) while fig. 10 shows the relationship between $\bar{P}$ and T. The T = 0 means that the DPHE is in a static state. For each Reynold number, the $\bar{K}$ was the highest at T = 5 seconds. When T = 5 seconds, compared to the $\bar{K}$ of the static

DPHE, the $\overline{K}$ of the oscillating DPHE increased by 4.53%, 2.44%, 1.78%, 1.47% and 1.27% for various Re_c. The $\overline{K}$ of the oscillating DPHE increased by 1.78%, 0.54%, 0.70%, 1.10% and 1.28% for various Re_h. Similarly, the $\overline{P}$ was the highest at $T = 5$ seconds. Compared to the P of the static DPHE, the $\overline{P}$ of the oscillating DPHE increased by 9.74%, 3.55%, 1.66%, 0.97% and 0.65 % for various Re_c. The $\overline{P}$ increased by 1.66%, 1.62%, 1.47%, 1.27%, and 1.06% for various Re_h compared to the stable DPHE.

Figure 9 illustrates that changing the oscillation period has little effect on the $\overline{K}$ of the DPHE. The effect of the oscillation period on the $\overline{K}$ of the DPHE becomes smaller as the Reynolds number increases. Figure 10 demonstrates that the effect of the oscillation period on $\overline{P}$ of DPHE becomes smaller as the Reynolds number increases. The $\overline{P}$ increases as T becomes shorter. Whilst the highest $\overline{P}$ of the outer tube appears at $T = 5$ seconds.

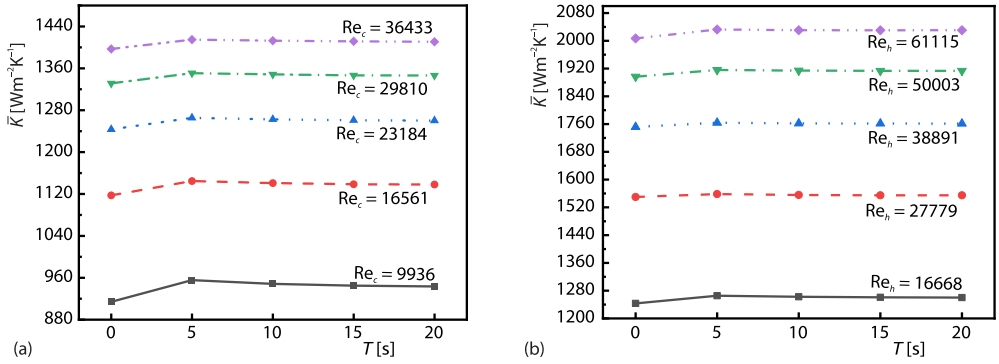

Figure 9. Variation of $\overline{K}$ with various T; (a) average total heat transfer coefficient when Re_{eh} = 16668 and (b) average total heat transfer coefficient when Re_c = 23184

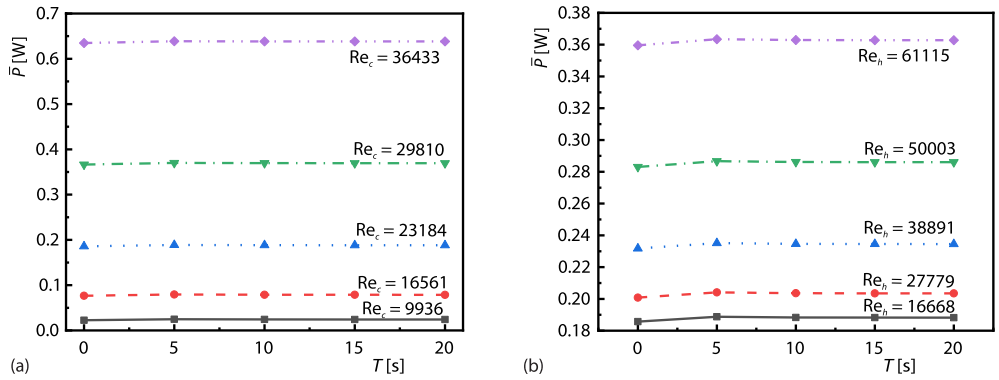

Figure 10. Variation of $\overline{P}$ with various T; (a) average pump power when Re_h = 16668 and (b) average pump power when Re_c = 23184

Thermal performance of the inner and outer side

Heat transfer and pressure drop are important parameters in heat exchanger design. It is desirable to obtain a lower pressure drop at the highest heat transfer rate. To quantify the enhanced heat transfer indicator of the inner and outer tubes of DPHE, the equation can be used [4]:

$$\eta = \frac{(\overline{Nu_o} / \overline{Nu_s})}{(f_o / f_s)^{1/3}} \tag{17}$$

Figure 11 shows the relationship between heat transfer performance η and various amplitudes under ten different Reynolds number when the $T = 10$ seconds. Figure 12 shows the variation of η with varying periods when $A = 0.5$ rad/s. The effect of oscillatory motion on the heat transfer performance of DPHE inner and outer tubes differs.

When $T = 10$ s, for $A \leq 0.5$ rad/s, the thermal performance of the outer tubes all obtain a small improvement. When $A \geq 0.5$ rad/s, the η of the outer tubes with low Re_c (Re_c = 9936, Re_c = 16561) decreases with the increase of A, which indicated that the enhancement effect of heat exchanger obtained by increasing amplitude was less than the pressure drop loss, resulting in the deterioration of thermal performance. The lowest η is taken to be 0.974 at A = 1 rad/s, Re_c = 9936. The f of outer tube with high Reynolds number (Re_c = 23184, Re_c = 29810, Re_c = 36433) is less affected by A and its efficiency remains essentially invariant. The thermal performance of the inner tube is the opposite of the outer tube. When $A \geq 0.5$ rad/s, the η of the inner tubes with low Reynolds number (Re_c = 16668, Re_c = 27779) increases with the increase of A. The highest η is taken to be 1.0502 at A = 1 rad/s, Re_c = 16668. The η of the inner tubes with high Reynolds number (Re_c = 38891, Re_c = 50003, Re_c = 61115) decreases with the increase of A. The lowest η is taken to be 0.978 at A = 1 rad/s, Re_c = 38891.

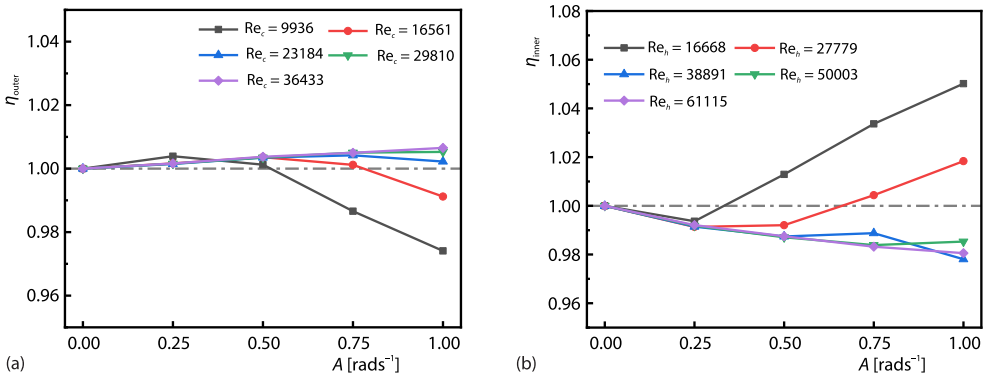

Figure 11. Variation of η with various A; (a) thermal performance when Re_h = 16668 and (b) thermal performance when Re_c = 23184

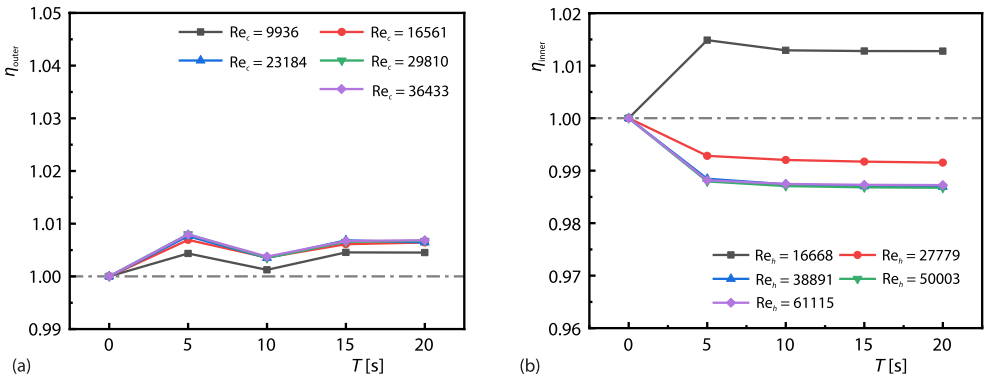

Figure 12. Variation of η with various T; (a) thermal performance when Re_h = 16668 and (b) thermal performance when Rec = 23184

Compared with the η of the static DPHE, when $A = 0.5$ rad/s and $T = 5$ seconds, the η of the outer tubes increase by 0.43%, 0.69%, 0.76%, 0.80%, and 0.80%. Differently, the η

of the inner tube reaches the maximum value of the oscillatory state when A = 0.5 rad/s and T = 5 seconds, varying by 1.48%, –0.71%, –1.15%, –1.20%, and –1.18%, respectively, and then remained almost unchanged with the increase of T. It is shown from the fig. 2 that the thermal performance of the DPHE could not be changed by continuously increasing the period under this condition. It indicates that the period variation of the oscillatory motion has little effect on the thermal performance. The thermal performance of the heat exchanger can be optimized by appropriately reducing the inlet Reynolds number of the inner tube.

Conclusions

In this paper, a DPHE in a static state and periodic cosine oscillation state are numerically studied. The effects of amplitude (A = 0.25 rad/s, 0.5 rad/s, 0.75 rad/s, and 1.0 rad/s) and period (T = 5 seconds, 10 seconds, 15 seconds, and 20 seconds) are investigated when the Re_h in the inner tube is constant at 16668 and the outer tube is varied at 9936, 16561, 23184, 29180, and 36433. Furthermore, analysis is performed when the Re_c in the outer tube is constant at 23184 and the inner tube is varied at 16668, 27779, 38891, 50003, and 61115. The main conclusions are as follows.

- The periodic oscillation motion enhances the fluid turbulence in the casing heat exchanger, thins the boundary-layer, enhances the heat transfer effect, but also creates a high pump power.
- In the periodic motion state, the heat transfer and pressure drop of the heat exchanger also have periodic laws, and the period is half that of the periodic motion of the heat exchanger. The changes of heat transfer and pressure drop are not synchronous with the periodic oscillation.
- For low Reynolds number, the heat transfer enhancement by oscillatory motion is more pronounced. The total heat transfer coefficient of DPHE is improved by up to 9.84%. While for high Reynolds number, the total heat transfer coefficient of DPHE increased by only 2.32%. The pump power of DPHE under oscillation is positively related to its Reynolds number and amplitude and negatively related to its period.
- When the amplitude exceeds 0.5 rad/s, the oscillation condition has thermal performance enhancement for the inner tube with low Reynolds number and the outer tube with high Reynolds number. The change of oscillation period has little effect on the thermal performance. In general, the thermal performance of the inner and outer tubes is better when the period is smaller.

Acknowledgment

This research was funded by Postgraduate Research & Practice Innovation Program of Jiangsu Province (Project reference No. KYCX22-1309).

The computational resources generously provided by the High Performance Computing Center of Nanjing Tech University are greatly appreciated.

Nomenclature

A – amplitude, [rads^{-1}]
c_p – specific heat capacity of fluid, [Jkg^{-1}K^{-1}]
D – equivalent diameter of outer pipe, [mm]
f – fraction factor
h – heat transfer coefficient, [Wm^{-2}K^{-1}]
K – total heat transfer coefficient, [Wm^{-2}K^{-1}]
$\bar{K}$ – average total heat transfer coefficient, [Wm^{-2}K^{-1}]
L – length of the tube, [mm]
Nu – Nusselt number (=hD_e/λ)
p – pressure, [Pa]
P – pump power, [W]

$\bar{P}$ – average pump power, [W]
Q – heat transfer quantity, [W]
q_m – mass-flow rate, [kgs^{-1}]
q_v – volume flow rate, [m^{3}s^{-1}]
Re – Reynolds number (=$\rho VD_e/\mu$)
S – total heat transfer area, [m^2]
T – period, [s]
u, v, w – direction of co-ordinate
V – velocity, [ms^{-1}]

Greek symbols

ε – turbulence energy dissipation rate
η – thermal performance
λ – thermal conductivity, [Wm^{-1}K^{-1}]
μ – dynamic viscosity, [Pa·s]
μ_e – effective viscosity, [Pa·s]
ρ – fluid density, [kgm^{-3}]
τ – flow time, [s]
ω – angular velocity, [rads^{-1}]

Subscripts

c – cold water
e – equivalent
h – hot water
in – inlet
inner – inner tube
max – maximum value in periodic variation
min – minimum value in periodic variation
o – periodic oscillation
out – outlet
outer – vouter tube
s – static state
t – turbulence
wall – tube wall

Acronyms

DPHE – double-pipe heat exchanger
LMTD – logarithmic mean temperature difference, [K]

References

[1] Ishida, I., *et al*., Thermal-Hydraulic Behavior of A Marine Reactor during Oscillations, *Nuclear Engineering and Design*, *120* (1990), 2, pp. 213-225
[2] Vaezi, S., *et al*., Effect of Aspect Ratio on Heat Transfer Enhancement in Alternating Oval Double Pipe Heat Exchangers, *Applied Thermal Engineering*, *125* (2017), Oct., pp. 1164-1172
[3] Riesner, M., *et al*., Rankine Source Time Domain Method for Non-Linear Ship Motions in Steep Oblique Waves, *Ships and Offshore Structures*, *14* (2019), 3, pp. 295-308
[4] Hashemian, M., *et al*., Enhancement of Heat Transfer Rate with Structural Modification of Double Pipe Heat Exchanger by Changing Cylindrical Form of Tubes into Conical Form, *Applied Thermal Engineering*, *118* (2017), May, pp. 408-417
[5] Huu-Quan, D., *et al*., The 3-D Numerical Investigation of Turbulent Forced Convection in a Double-Pipe Heat Exchanger with Flat Inner Pipe, *Applied Thermal Engineering*, *182* (2021), 116106
[6] El Maakoul, A., *et al*., Numerical Investigation of Thermohydraulic Performance of Air to Water Double-Pipe Heat Exchanger with Helical Fins, *Applied Thermal Engineering*, *127* (2017), Dec., pp. 127-139
[7] Sharifi, K., *et al*., Computational Fluid Dynamics (CFD) Technique to Study the Effects of Helical Wire Inserts on Heat Transfer and Pressure Drop in a Double Pipe Heat Exchanger, *Applied Thermal Engineering*, *128* (2018), Jan., pp. 898-910
[8] Aly, W. I. A., Numerical Study on Turbulent Heat Transfer and Pressure Drop of Nanofluid in Coiled Tube-in-Tube Heat Exchangers, *Energy Conversion and Management*, *79* (2014), Mar., pp. 304-316
[9] Darzi, A. A. R., *et al*., Heat Transfer and Flow Characteristics of AL_2O_3-Water Nanofluid in a Double Tube Heat Exchanger, *International Communications in Heat and Mass Transfer*, *47* (2013), Oct., pp. 105-112
[10] Xu, H. J., *et al*., Numerical Investigation on Self-Coupling Heat Transfer in a Counter-Flow Double-Pipe Heat Exchanger Filled with Metallic Foams, *Applied Thermal Engineering*, *66* (2014), 1, pp. 43-54
[11] Pendyala, R., *et al*., Flow and Pressure Drop Fluctuations in a Vertical Tube Subject to Low Frequency Oscillations, *Nuclear Engineering and Design*, *238* (2008), Jan., pp. 178-187
[12] Tian, W., *et al*., Experimental Study of Single-Phase Natural Circulation Heat Transfer in a Narrow, Vertical, Rectangular Channel under Rolling Motion Conditions, *International Journal of Heat and Mass Transfer*, *107* (2017), Apr., pp. 592-606
[13] Wang, C., *et al*., Experimental Study of Single-Phase Forced Circulation Heat Transfer in Circular Pipe under Rolling Motion, *Nuclear Engineering and Design*, *265* (2013), Dec., pp. 348-355
[14] Chen, C., *et al*., Heat Transfer Characteristics of Oscillating Flow in A Narrow Channel under Rolling Motion, *Annals of Nuclear Energy*, *110* (2017), Dec., pp. 668-678
[15] Bagherzadeh, B. C., Javadi, K., Flow Control around a Circular Cylinder with Swinging Thin Plates, *Journal of Fluids and Structures*, *81* (2018), Aug., pp. 738-760
[16] Rahman, A., Tafti, D., Characterization of Heat Transfer Enhancement for an Oscillating Flat Plate-Fin, *International Journal of Heat and Mass Transfer*, *147* (2020), 119001

[17] Yang, Y.-T., Chen, C.-H., Numerical Simulation of Turbulent Fluid-Flow and Heat Transfer Characteristics of Heated Blocks in the Channel with an Oscillating Cylinder, *International Journal of Heat and Mass Transfer*, *51* (2008), 7, pp. 1603-1612
[18] Rui, L., Tao, H., Numerical Investigation of Heat Transfer and Flow Inner Tube with Periodically Cosine Oscillation, *International Journal of Heat and Mass Transfe*r, *127* (2018), Dec., pp. 1082-1091
[19] Hashemian, M., *et al*., A Comprehensive Numerical Study on Multi-Criteria Design Analyses in a Novel Form (Conical) of Double Pipe Heat Exchanger, Applied Thermal Engineering, *102* (2016), June, pp. 1228-1237
[20] Yan B., *et al*., Research on Operational Characteristics of Passive Residual Heat Removal System under Rolling Motion, *Nuclear Engineering and Design*, *239* (2009), 11, pp. 2302-2310
[21] Yan, B. H., Review of the Nuclear Reactor Thermal Hydraulic Research in Ocean Motions, *Nuclear Engineering and Design*, *313* (2017), Mar., pp. 370-385
[22] Patankar, S. V., *Numerical Heat Transfer and Fluid-Flow*, Hemisphere Publ. Corp., New York, USA, 1980, vol. 58, p. 288
[23] Tao, H., *et al*., Numerical Study on Effect of Oscillation Center Position on Heat Transfer and Flow Internal Tube, *International Journal of Heat and Mass Transfer*, *137* (2019), Jul., pp. 799-808
[24] Gnielinski, V., New Equations For Heat and Mass Transfer in Turbulent Pipe and Channel Flow, *Int. Chem. Eng*., *16* (1976), 2, pp. 359-368
[25] Courant, R., *et al*., On the Partial Difference Equations of Mathematical Physics, *IBM Journal of Research and Development*, *11* (1967), 2, pp. 215-234
[26] Shchepetkin, A. F., An Adaptive, Courant-Number-Dependent Implicit Scheme for Vertical Advection in Oceanic Modelling, *Ocean Modelling*, *91* (2015), July, pp. 38-69
[27] Han, H.-Z., *et al.*, Multi-Objective Shape Optimization of Double Pipe Heat Exchanger with Inner Corrugated Tube Using RSM Method, *International Journal of Thermal Sciences*, *90* (2015), Apr., pp. 173-186

Paper submitted: February 1, 2023
Paper revised: April 7, 2023
Paper accepted: April 24, 2023